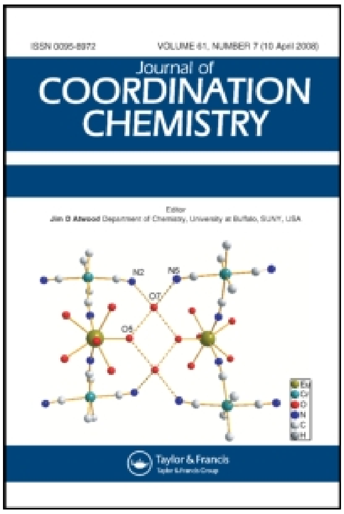

Journal of Coordination Chemistry
Publication details, including instructions for authors and subscription information:
http://www.informaworld.com/smpp/title~content=t713455674

Preparation, structural characterization, and thermal behaviors of Nd(III) compounds derived from 3,5-dinitropyridone

Jun-Ge Wang[ab]; Qiu-Ping Zhou[ab]; Guo-Fang Zhang[ab]; Ping Li[ab]; Bao-Hua Chen[c]; Feng-Qi Zhao[d]; Ji-Zhen Li[d]; Xue-Zhong Fan[d]

[a] Key Laboratory of Applied Surface and Colloid Chemistry, Shaanxi Normal University, Xi'an 710062, P.R. China [b] School of Chemistry and Materials Science, Shaanxi Normal University, Xi'an 710062, P.R. China [c] Xi'an Power Resin Factory, Xi'an 710038, P.R. China [d] Xi'an Modern Chemistry Research Institute, Xi'an 710065, P.R. China

To cite this Article Wang, Jun-Ge , Zhou, Qiu-Ping , Zhang, Guo-Fang , Li, Ping , Chen, Bao-Hua , Zhao, Feng-Qi , Li, Ji-Zhen and Fan, Xue-Zhong(2010) 'Preparation, structural characterization, and thermal behaviors of Nd(III) compounds derived from 3,5-dinitropyridone', Journal of Coordination Chemistry, 63: 8, 1379 — 1389, First published on: 20 April 2010 (iFirst)

To link to this Article: DOI: 10.1080/00958971003786625

URL: http://dx.doi.org/10.1080/00958971003786625

Journal of Coordination Chemistry
Vol. 63, No. 8, 20 April 2010, 1379–1389

Taylor & Francis
Taylor & Francis Group

Preparation, structural characterization, and thermal behaviors of Nd(III) compounds derived from 3,5-dinitropyridone

JUN-GE WANG†‡, QIU-PING ZHOU†‡, GUO-FANG ZHANG*†‡, PING LI†‡,
BAO-HUA CHEN§, FENG-QI ZHAO¶, JI-ZHEN LI¶ and XUE-ZHONG FAN¶

†Key Laboratory of Applied Surface and Colloid Chemistry, Shaanxi Normal University,
Ministry of Education, Xi'an 710062, P.R. China
‡School of Chemistry and Materials Science, Shaanxi Normal University,
Xi'an 710062, P.R. China
§Xi'an Power Resin Factory, Xi'an 710038, P.R. China
¶Xi'an Modern Chemistry Research Institute, Xi'an 710065, P.R. China

(*Received 10 October 2009; in final form 23 December 2009*)

Three neodymium compounds, $Nd(4DNP)_3(C_2H_5OH)_3$ (**1**), $Nd(4DNPO)_3 \cdot 7H_2O$ (**2**), and $\{[Nd(\mu\text{-ox})(4DNPO)(H_2O)_4] \cdot 4H_2O\}_n$ (**3**) (4HDNP, 3,5-dinitropyrid-4-one; 4HDNPO, 3,5-dinitropyrid-4-one-*N*-hydroxide; ox, oxalate), were synthesized and characterized by FT-IR, elemental analysis, thermogravimetry–differential scanning calorimetry (TG–DSC), and two of them by single-crystal X-ray diffraction analyses. The results revealed that in **1**, the Nd(III) is surrounded by three chelating ligands and three ethanol solvent molecules. The structure of **3** could be described as 1-D chains in which Nd is bis-bidentately bridged by oxalates, together with a monodentate 3,5-dinitropyrid-4-onate N-oxide 4DNPO ligand and four water molecules as well as four uncoordinated water molecules in the crystal lattice. The origin of the oxalate anions in **3** is probably due to decomposition of the 4DNPO or its oxidation of other species. The TG–DTG (DTG, derivative thermogravimetry) and DSC analyses showed that **1** underwent a three-stage decomposition process. A kinetic equation for decomposition reaction of **2** was also obtained. The apparent activation energy (E_a) and pre-exponential factor (A) of the main decomposition reaction are $157.70\,\mathrm{kJ\,mol^{-1}}$ and $10^{11.97}\,\mathrm{s^{-1}}$, respectively. The kinetic equation can thus be expressed as $d\alpha/dt = 10^{11.97}(1-\alpha)e^{-1.90 \times 10^4/T}$.

Keywords: Neodymium complex; 3,5-Dinitropyridone; Crystal structure; Thermal behavior; Kinetics

1. Introduction

Rare-earth metal complexes continue to be the focus of much research due to their remarkable physical properties and applications as magnetic functional materials, electroluminescent devices, catalysis, zeolite-like materials, and luminescent probes or labels in biological systems [1]. The knowledge of their structures is of importance for an understanding of their properties. The coordination number of trivalent lanthanide ions is from 6 to 10 since they have different ionic radii and electronic configurations [1, 2].

---

*Corresponding author. Email: gfzhang@snnu.edu.cn

Journal of Coordination Chemistry
ISSN 0095-8972 print/ISSN 1029-0389 online © 2010 Taylor & Francis
DOI: 10.1080/00958971003786625

Much attention has been focused on energetic catalysts, which usually contain nitro groups on the molecule, in order to adjust the trajectory properties of solid propellants. In the case of energetic catalysts in two-base propellants, metal salts, particularly copper, and lead salts of polynitrophenols [3], picric acids [4], and 3-nitro-1,2,4-triazole-5-one (NTO) [5] have been extensively studied. In contrast, few metal salts of polynitropyridone derivatives have been investigated and no crystal structures have been reported until we began to study their molecular structures and thermodecomposition behaviors [6], while polynitropyridone derivatives are found in many other applications [7]. To date, crystal structures of two Pb(II) and Cu(II) salts and a number of alkali and alkaline-earth metals as well as a few transition-metal salts derived from three kinds of dinitropyridone ligands, i.e., 2(4)-hydroxyl-3,5-dinitropyridine(-*N*-oxide) (2HDNP, 4HDNP, and 4HDNPO), have been determined and their thermodecomposition behaviors investigated in our group [8]. Up to now, rare-earth metal complexes as catalysts employed in solid propellants and their crystal structures have rarely been studied [5a, 5b]. As an extension of our work on polynitropyridone materials, we focused our attention on lanthanide compounds derived from 3,5-dinitropyridone and on the exploration of their crystal structures and thermal decomposition behavior. Here, we report on the synthesis, structural characterization, thermal behaviors, and non-isothermal decomposition reaction kinetics of neodymium compounds of 3,5-dinitropyridone.

2. Experimental

2.1. *Materials and physical measurements*

The two ligands, 4-hydroxyl-3,5-dinitro-pyridine (4HDNP) and 4-hydroxyl-3,5-dinitropyridine-*N*-oxide (4HDNPO), were synthesized following the methods previously described with slight modification [9]. Other reagents are commercially available and were used without purification. All experiments were carried out in doubly distilled water.

IR spectra of the complexes were recorded on a Perkin Elmer FT-IR spectrophotometer from 4000–400 cm^{-1} using KBr pellets. Elemental content of carbon, hydrogen, and nitrogen were determined by a German Vario EL III analyzer. The contents of Nd were determined by a JY-38 Plus ICP spectrometer. The crystal structure was determined with a Bruker Smart-1000 CCD diffractometer. The thermogravimetry–derivative thermogravimetry (TG–DTG) curves and differential scanning calorimetry (DSC) curves were obtained with a Model TGA 2950 thermobalance and a Model DSC 190S differential scanning calorimeter made by American TA Company. The conditions were sample mass, less than 1.00 mg; heating rate, 10°C min^{-1}; atmosphere, flowing N_2 gas.

2.2. *Synthesis*

2.2.1. $Nd(4DNP)_3(C_2H_5OH)_3$, (1). Equal molar ratio of LiOH (0.42 g, 10 mmol) and 4HDNP (1.85 g, 10 mmol) were added in 60 mL doubly distilled water at 60°C and stirred for 1 h to get corresponding lithium salts, to which one-third molar ratio of $Nd(NO_3)_3 \cdot 6H_2O$ (1.46 g, 3.33 mmol) was added dropwise and the reaction was maintained for 2 h with the formation of pale yellow–green precipitate. After evaporation of the water under vacuum, the residue was recrystallized in anhydrous ethanol to afford the desired product (yield: 1.65 g, 71.2%). Anal. Calcd for $C_{21}H_{24}N_9NdO_{18}$, **1** (%): C, 30.22; H, 2.90; N, 15.10; and Nd, 17.28. Found: C, 29.72; H, 2.83; N, 14.77; and Nd, 17.42. Crystals of **1** suitable for single-crystal X-ray diffraction analysis were obtained by slow evaporation of its anhydrous ethanolic solution for 4 weeks. FT-IR (KBr, cm^{-1}): 1616, s, ν(C=O); 1546, s, ν_{asym}(N–O); 1487, s, ν(C=C); 1357, s, ν_{sym}(N–O); 1283, m, ν(C–N).

2.2.2. ($Nd(4DNPO)_3 \cdot 7H_2O$), (2). A similar synthetic procedure to that of **1** was used for the preparation of **2**. The isolated pale yellow–green precipitate was recrystallized from water to afford a product with a yield of 81.4%. Anal. Calcd for $C_{15}H_{20}N_9NdO_{25}$, **2** (%): C, 20.69; H, 2.32; N, 14.48; and Nd, 16.57. Found: C, 19.93; H, 2.17; N, 13.74; and Nd, 16.84. FT-IR (KBr, cm^{-1}): 1670, s, ν(C=O); 1577, s, ν_{asym}(N–O); 1456, s, ν(C=C); 1348, s, ν_{sym}(N–O); 1266, m, ν(C–N).

2.2.3. $\{[Nd(\mu\text{-ox})(4DNPO)(H_2O)_4] \cdot 4H_2O\}_n$, (3). Crystals of **3** were collected by slow evaporation of an aqueous solution of compound **2** for 4 months with a yield of 34.2%. Anal. Calcd for $C_7H_{18}N_3NdO_{18}$, **3** (%): C, 14.58; H, 3.15; N, 7.29; and Nd, 25.02. Found: C, 14.63; H, 2.77; N, 7.85; and Nd, 24.72. FT-IR (KBr, cm^{-1}): 1668, s, ν(C=O); 1614, s, ν(C=O for $C_2O_4^{2-}$); 1584, s, ν_{asym}(N–O); 1466, s, ν(C=C); 1341, s, ν_{sym}(N–O); 1258, m, ν(C–N).

2.3. *X-ray diffraction analysis*

A single crystal of **1** or **3** was coated with epoxy glue in order to prevent spontaneous liberation of solvent molecules from the specimen under ambient conditions. Determination of the unit cell and data collection for **1** and **3** were performed on a Bruker Smart-1000 CCD diffractometer with graphite monochromated Mo-Kα radiation ($\lambda = 0.71073$ Å) using ω–2θ scan technique. The structures were solved by direct methods and refined on F^2 by full matrix least-squares with the Bruker's SHELXL-97 program [10]. All non-hydrogen atoms were refined anisotropically. All hydrogens were treated using a riding model. Data collection details and structure determination results are summarized in table 1. Selected bond lengths and angles are given in table 2.

3. Results and discussion

3.1. *Crystal structure of $Nd(4DNP)_3(C_2H_5OH)_3$ (1)*

Molecular structure of **1** is illustrated in figure 1. The structural feature of **1** is the presence of three 4DNP ligands bidentate coordinated to Nd(III). The Nd(III) is coordinated to nine oxygens, three from ethanol (O16, O17, and O18). The Nd–$O_{ethanol}$

Table 1. Crystal data and structure refinement data for the neodymium **1** and **3**.

Compound	**1**	**3**
Empirical formula	$C_{21}H_{24}N_9NdO_{18}$	$C_7H_{18}N_3NdO_{18}$
Formula weight	834.73	576.48
Crystal system	Monoclinic	Triclinic
Space group	$P2(1)/c$	$P\bar{1}$
Unit cell dimensions (Å, °)		
a	15.256(4)	6.7695(7)
b	10.737(2)	9.9695(11)
c	19.200(4)	14.6269(16)
α	90	73.7190(10)
β	95.594(2)	88.1370(10)
γ	90	76.6930(10)
Volume (Å^3), Z	3130.2(12), 4	921.58(17), 2
Calculated density (g cm^{-3})	1.771	2.077
Absorption coefficient (mm^{-1})	1.753	2.916
$F(0\,0\,0)$	1668	570
Crystal size (mm^3)	$0.39 \times 0.25 \times 0.21$	$0.37 \times 0.26 \times 0.07$
θ range for data collection (°)	2.32–27.50	2.26–25.50
Limiting indices	$-19 < h < 19$, $-13 < k < 13$, $-24 < l < 24$	$-8 < h < 8$, $-12 < k < 12$, $-17 < l < 17$
Reflections collected	27,003	6844
Independent reflection	7175 [R(int) = 0.0195]	3396 [R(int) = 0.0146]
Data/restraints/parameters	6217/459/444	3297/12/262
Goodness-of-fit on F^2	1.050	1.111
Final R indices [$I > 2\sigma(I)$]	$R_1 = 0.0294$, $wR_2 = 0.0822$	$R_1 = 0.0185$, $wR_2 = 0.0471$
R indices (all data)	$R_1 = 0.0358$, $wR_2 = 0.0877$	$R_1 = 0.0191$, $wR_2 = 0.0477$
Largest difference peak and hole (e Å^{-3})	0.582 and −0.768	0.450 and −0.799

bond distances are within the range 2.453(2)–2.501(2) Å, longer than the sum of the covalent radii of the Nd and O atoms (2.37 Å), indicating a relatively weak interaction between the solvent and the metal ion. The Nd(III) forms three six-membered chelate rings with 4DNP ligands by an oxygen of one nitro group and the oxygen of the pyridonate group.

The Nd–O distances to the nitro groups are in the range 2.606(3)–2.646(3) Å, indicating that the Nd–O bonds to the nitro groups are also relatively weak, as observed in [$La_2(2,6\text{-DNP})_6(H_2O)_4$] [5b]. The Nd–O bond distances to the pyridonate groups are in the range 2.360(2)–2.395(2) Å (table 2), which are comparable to those reported for other Ln(III) compounds [11]. In addition, the calculated dihedral angles between the pyridine rings and the coordinated nitro groups support the evidence for an interaction between the oxygens on the nitro groups and the Nd. The dihedral angle between the pyridine rings and the coordinated nitro groups are in the range 4.8(5)–17.6(3) Å for the coordinated nitro groups and 25.0(6)–87.4(5) Å for the uncoordinated nitro groups. The closest distance between the oxygens of the uncoordinated nitro groups and the Nd is longer than 4.7 Å.

There are hydrogen bonds between the three ethanols and the nitrogens on the pyridine rings of the ligands: O(16)–H(16D)$\cdots$N(4)$^{\#3}$ 2.745(4) Å, 154.8 Å; O(17) – H(17D)$\cdots$N(1)$^{\#2}$ 2.675(4) Å, 167.4 Å; O(18)–H(18D)$\cdots$N(7)$^{\#1}$ 2.664(4) Å, 174.4 Å ($^{\#1}$:$-x+1$, $y-1/2$, $-z+1/2$; $^{\#2}$: x, $-y+3/2$, $z+1/2$; $^{\#3}$: $-x$, $y-1/2$, $-z+1/2$).

Figure 2 shows the coordination polyhedron of Nd(III) in **1**. The skeletal structure around the Nd atom can be described as a distorted tricapped trigonal prism, similar in

Table 2. Selected bond lengths (Å) and angles (°) for **1** and **3**.

1		**3**	
Nd(1)–O(1)	2.381(2)	Nd(1)–O(4)	2.4798(18)
Nd(1)–O(2)	2.606(3)	Nd(1)–O(16)$^{\#1}$	2.4891(19)
Nd(1)–O(6)	2.360(2)	Nd(1)–O(18)$^{\#2}$	2.4974(19)
Nd(1)–O(7)	2.646(3)	Nd(1)–O(1)	2.509(2)
Nd(1)–O(11)	2.395(2)	Nd(1)–O(17)	2.5123(19)
Nd(1)–O(12)	2.606(3)	Nd(1)–O(3)	2.5153(19)
Nd(1)–O(16)	2.501(2)	Nd(1)–O(15)	2.5246(18)
Nd(1)–O(17)	2.460(2)	Nd(1)–O(2)	2.525(2)
Nd(1)–O(18)	2.453(2)	Nd(1)–O(9)	2.5254(19)
O(1)–Nd(1)–O(16)	83.21(9)	O(4)–Nd(1)–O(16)$^{\#1}$	135.33(6)
O(1)–Nd(1)–O(17)	139.09(8)	O(4)–Nd(1)–O(18)$^{\#2}$	131.02(7)
O(1)–Nd(1)–O(18)	136.23(9)	O(16)$^{\#1}$–Nd(1)–O(18)$^{\#2}$	70.29(7)
O(2)–Nd(1)–O(12)	120.04(10)	O(4)–Nd(1)–O(1)	91.39(7)
O(2)–Nd(1)–O(7)	121.19(8)	O(16)$^{\#1}$–Nd(1)–O(1)	81.86(7)
O(6)–Nd(1)–O(1)	77.86(9)	O(18)$^{\#2}$–Nd(1)–O(1)	137.44(7)
O(6)–Nd(1)–O(2)	134.03(9)	O(4)–Nd(1)–O(17)	148.47(7)
O(6)–Nd(1)–O(7)	65.83(8)	O(16)$^{\#1}$–Nd(1)–O(17)	72.57(7)
O(6)–Nd(1)–O(11)	79.46(10)	O(18)$^{\#2}$–Nd(1)–O(17)	64.60(6)
O(6)–Nd(1)–O(12)	68.75(10)	O(1)–Nd(1)–O(17)	76.88(7)
O(6)–Nd(1)–O(16)	133.19(9)	O(4)–Nd(1)–O(3)	73.71(7)
O(6)–Nd(1)–O(17)	85.62(9)	O(16)$^{\#1}$–Nd(1)–O(3)	139.33(7)
O(6)–Nd(1)–O(18)	140.51(10)	O(18)$^{\#2}$–Nd(1)–O(3)	69.15(7)
O(11)–Nd(1)–O(2)	67.92(9)	O(1)–Nd(1)–O(3)	132.58(7)
O(11)–Nd(1)–O(7)	137.82(9)	O(17)–Nd(1)–O(3)	92.70(7)
O(11)–Nd(1)–O(12)	65.05(9)	O(4)–Nd(1)–O(15)	71.60(6)
O(11)–Nd(1)–O(16)	138.30(9)	O(16)$^{\#1}$–Nd(1)–O(15)	64.99(6)
O(11)–Nd(1)–O(17)	133.68(9)	O(18)$^{\#2}$–Nd(1)–O(15)	122.97(6)
O(11)–Nd(1)–O(18)	87.34(10)	O(1)–Nd(1)–O(15)	67.65(7)
O(12)–Nd(1)–O(7)	118.50(9)	O(17)–Nd(1)–O(15)	127.23(7)
O(16)–Nd(1)–O(2)	70.38(8)	O(3)–Nd(1)–O(15)	140.05(6)

Symmetry operation: $^{\#1}-x+1, -y+2, -z+1$; $^{\#2}-x+1, -y+1, -z+1$.

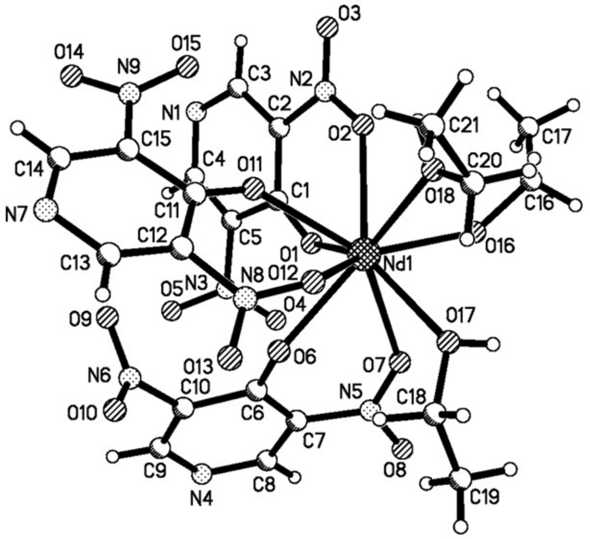

Figure 1. The molecular structure of Nd(4DNP)$_3$(C$_2$H$_5$OH)$_3$ (**1**) showing the scheme of atomic numbering.

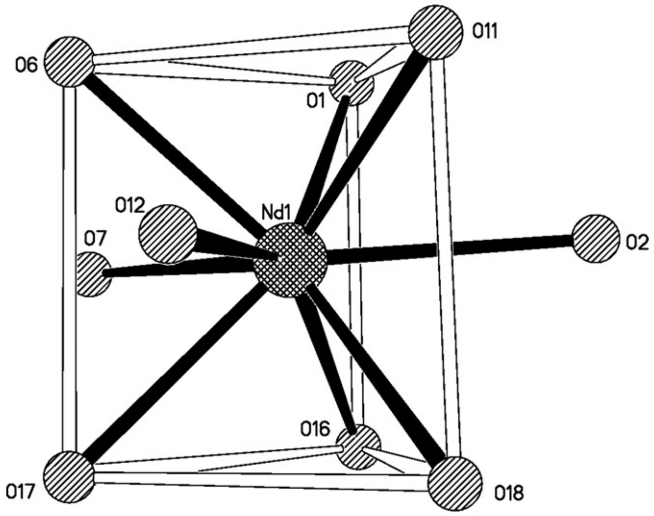

Figure 2. The coordination polyhedron of the Nd atom in Nd(4DNP)$_3$(C$_2$H$_5$OH)$_3$ (**1**). The tricapped trigonal prism is indicated by double solid lines.

structure to the Ln(III) in [Ln(NCS)$_3${(py)$_2$C(OEt)(OH)}$_3$] (Ln = Pr, Sm, and Gd) [11a]. Three ethanols coordinating directly to Nd(III) (O16, O17, and O18) occupy one basal site of the trigonal prism; three oxygens (O1, O6, and O11) from the pyridonate groups occupy another basal site of the prism. At relatively long distances, three oxygens (O2, O7, and O12) from the nitro groups of the ligands cap the sides of the trigonal prism.

3.2. *Crystal structure of {[Nd(μ-ox)(4DNPO) · (H$_2$O)$_4$] · 4H$_2$O}$_n$ (3)*

Figure 3 shows a fragment of the polymeric chain of **3**. The Nd compound could be described as 1-D zigzag chains in which the Nd atoms are bridged by centrosymmetric oxalate anions, contrasting in structure to the 3-D brick-wall framework in K[Gd(ox)(SO$_4$)(H$_2$O)] [12], in which the additional tridentate sulfate bridges extend the 1-D chain into a more complicated 3-D framework. One 4DNPO ligand and four water molecules coordinate with an Nd ion. There are four uncoordinated water molecules in the crystal lattice. So the formula of **3** should be correctly expressed as {[Nd(μ-ox)(4DNPO)(H$_2$O)$_4$] · 4H$_2$O}$_n$. The Nd–O$_{ox}$ bond distances are in the range 2.4798(18)–2.5254(19) Å (table 2), which are longer by ~0.1 Å than those in K[Gd(ox)(SO$_4$)(H$_2$O)] (the average Gd–O bond distance is 2.399 Å) [12], partly due to the lanthanide contraction. There is only one unique Nd in the asymmetric unit. Each oxalate in **3** is a *bis*-bidentate ligand, allowing it to bond with another Nd atom. As a result of oxalate bridging, the 1-D chain is formed.

There are abundant intra- and inter-molecular hydrogen bonds in the molecular structure of **3** due to the presence of water. The intermolecular hydrogen bonding between the 1-D chains, constructed by bridging oxalate groups, and crystalline water leads to the formation of a 3-D molecular network. These weak interactions contribute to the stabilization of the crystal structure.

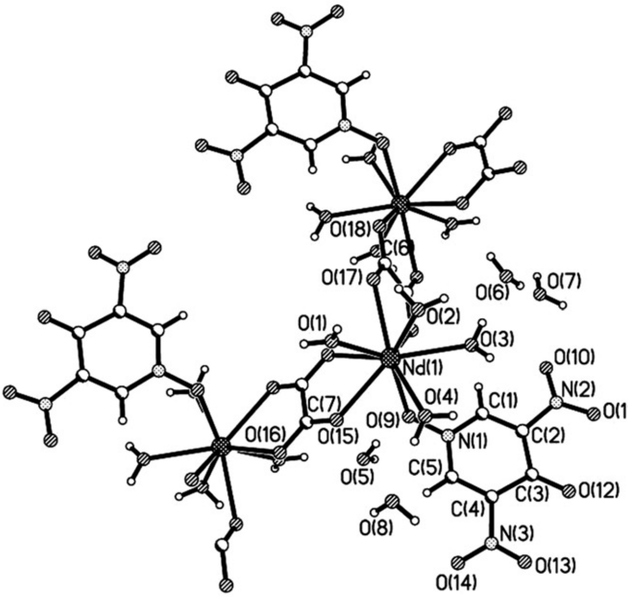

Figure 3. A perspective view of a fragment of the chain structure of $\{[\mathrm{Nd}(\mu\text{-ox})(4\mathrm{DNPO})(\mathrm{H_2O})_4]\cdot 4\mathrm{H_2O}\}_n$ (**3**), showing the asymmetric unit structure with the atom numbering scheme.

3.3. *FT-IR investigation on the formation of 3*

Compound **3**, as noted, was obtained during the crystal growth of **2** in water, without oxalate salt being used during the preparation and crystal growth. In order to verify the origin of the oxalate anions in **3**, we performed FT-IR spectrometry analysis of the isolated precipitate after different deposition times and of the crystal growth from water over different periods. As shown in figure 4, the IR spectra of the freshly isolated powder (a) and the samples after approximately 4 months storage in air (b) showed no distinct characteristic absorptions of chelating and/or bridging oxalate groups (its bending vibration at *ca* $1610\,\mathrm{cm^{-1}}$ and symmetric stretching vibration at *ca* $1350\,\mathrm{cm^{-1}}$ shielded by the symmetric stretching vibration of nitro groups), but in the IR spectrum of the powder after 8 months storage in air (c), the characteristic absorptions of oxalate groups are found (at $1614\,\mathrm{cm^{-1}}$), and absorption intensity becomes stronger in the crystals (d) collected from aqueous solution with similar wait [13]. These results revealed that the freshly prepared solid sample of **2** decomposes in air slowly and its aqueous solution underwent higher decomposition rate, leading to the formation of **3**. In order to verify our deduction, we investigated the reaction of $\mathrm{Nd(NO_3)_3\cdot 6H_2O}$, 4DNPOLi, and $\mathrm{Na_2C_2O_4}$. The first experiment is the simultaneous addition of both 4DNPOLi and $\mathrm{Na_2C_2O_4}$ aqueous solution to $\mathrm{Nd(NO_3)_3\cdot 6H_2O}$ aqueous solution, and the second experiment is the addition of $\mathrm{Na_2C_2O_4}$ to aqueous solution of $\mathrm{Nd(NO_3)_3\cdot 6H_2O}$ and 4DNPOLi after stirring at 60°C for 2 h. The isolated precipitates from both the experiments were recrystallized from anhydrous ethanol. The characterization revealed that the isolated precipitate from the first experiment was pure neodymium oxalate, verified by elemental and IR analyses, and only traces of neodymium(III) were detected from the corresponding filtrate; the powder afforded

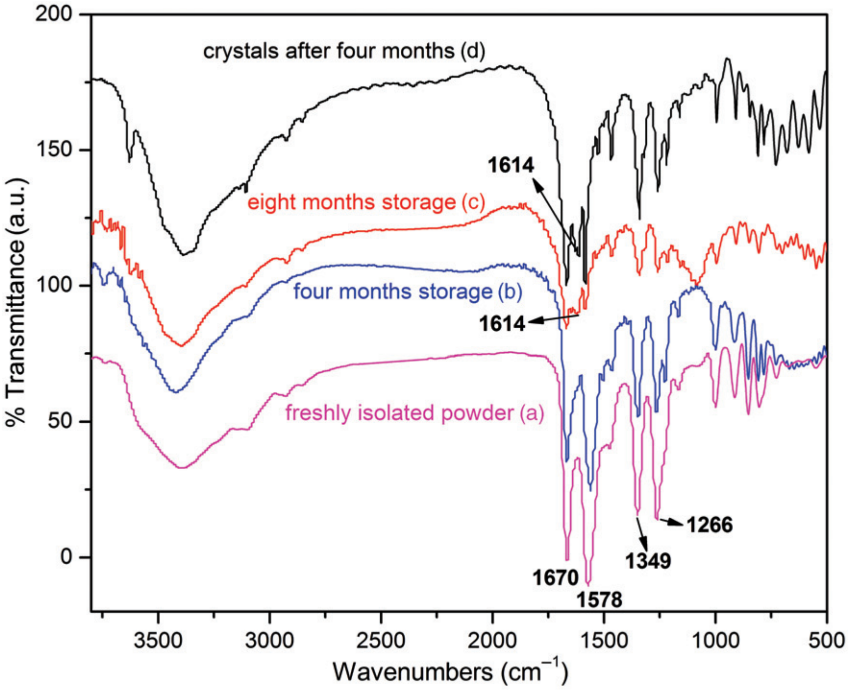

Figure 4. FT-IR spectrometry studies on the formation of **3** from **2** over different periods.

from the second experiment was a mixture and cannot be separated by common methods and therefore cannot be characterized. Nitroxides are generally unstable and undergo decomposition in the presence of light and wet air. Moreover, nitroxides have strong oxidizing properties. Therefore, instability and oxidizing property of 4DNPO could form the oxalate.

3.4. *Thermal analysis*

In order to evaluate the thermal stability of the synthesized compounds, TG–DTG and DSC experiments were used under N_2. Typical TG–DTG and DSC curves of **1** are shown in figures 5 and 6, respectively. The DSC curve shows two weak endothermic peaks (142.01°C and 179.31°C) and this endothermic course lasts from room temperature to higher than 200°C. There is an exothermic peak (339.74°C) before 430°C, and correspondingly there is a peak (321.56°C) on DTG curve. The decomposition process of $Nd(4DNP)_3(C_2H_5OH)_3$ could be divided into three stages: the first stage completes at 144.32°C accompanied with a 10.74% mass loss in agreement with the theoretical value of the mass loss of 10.78%, corresponding to the loss of $2C_2H_5OH$. The second stage of weight loss was caused by the loss of the third ethanol and all six nitro groups of the three ligand molecules, as we suggested for the thermal decomposition mechanism for $Pb(2DNP)_2$ [9d], accompanied with a 42.42% weight loss, which is in approximate agreement with the calculated value of 38.85%. The final stage ends at 571.42°C accompanied with a 26.01% mass loss, indicating

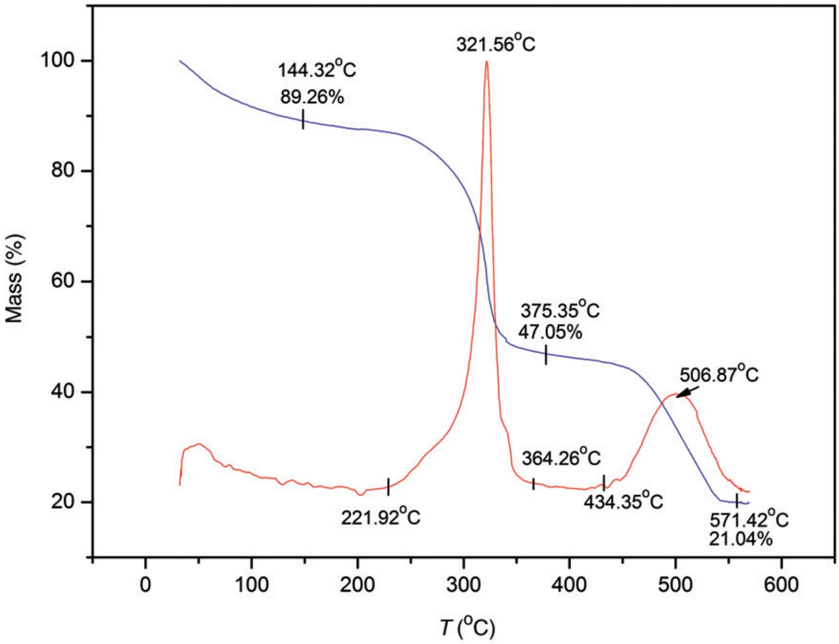

Figure 5. The TG–DTG curves for Nd(4DNP)$_3$(C$_2$H$_5$OH)$_3$ (**1**) at a heating rate of 10°C min^{-1}.

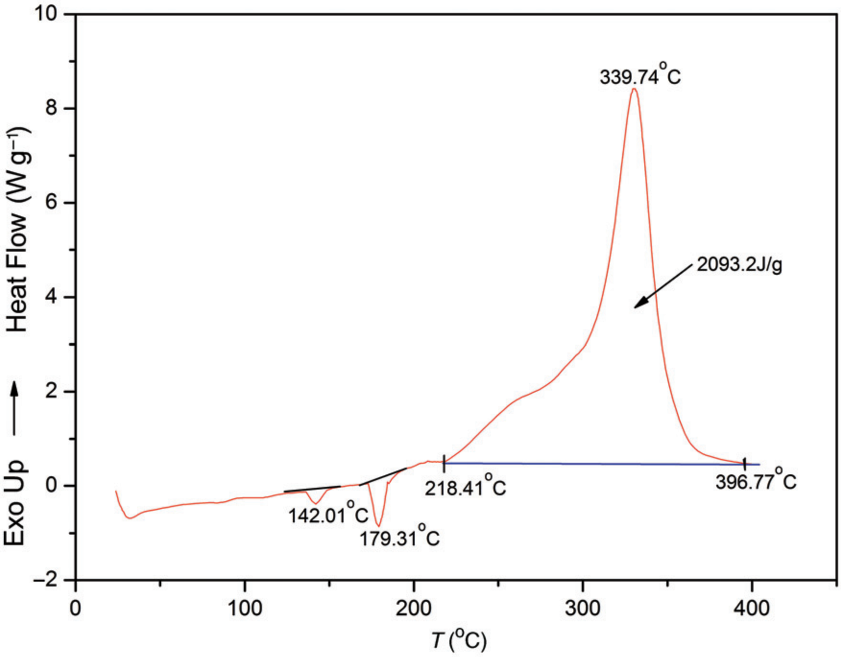

Figure 6. The DSC curve for Nd(4DNP)$_3$(C$_2$H$_5$OH)$_3$ (**1**) at a heating rate of 10°C min^{-1}.

complete decomposition of the intermediate into metal oxide, Nd_2O_3. During the exothermic process, the reaction heat is 2093.2 J g^{-1}. The decomposition peak of 4DNP ligand in **1** is at 339.74°C, *ca* 73°C higher than that of the free ligand 4HDNP (266.32°C), indicating that the binding of the ligand anion with neodymium(III) increases its thermal stability.

On the basis of the TG–DTG and DSC experiments and the calculated results, the pyrolysis mechanism for $Nd(4DNP)_3(C_2H_5OH)_3$ can be shown as follows:

$$\mathrm{Nd(4\,DNP)_3(C_2H_5OH)_3} \xrightarrow[40-144.32^{\circ}\mathrm{C}]{-2\mathrm{C_2H_5OH}} \mathrm{Nd(4\,DNP)_3(C_2H_5OH)} \xrightarrow[220-375.35^{\circ}\mathrm{C}]{-\mathrm{C_2H_5OH^+}\ \text{other fragment}} \xrightarrow[430-571.42^{\circ}\mathrm{C}]{\text{complete decomposition}} \mathrm{Nd_2O_3}$$

The most probable mechanism of the main decomposition of the Nd(III) compound **2** and the corresponding kinetic parameters (apparent activation energy (E_a kJ mol^{-1}), preexponential constant (A/s^{-1})) as well as the most probable kinetic model function were studied (Supplementary material). The results showed that the reaction mechanism of the exothermal decomposition process of **2** is controlled by Mample Law with $n = 1$, $G(\alpha) = -\ln(1-\alpha)$, and $f(\alpha) = (1-\alpha)$. E_a and A are 157.70 kJ mol^{-1} and $10^{11.97}$, respectively. The corresponding kinetic equation of the decomposition reaction of the Nd compound **2** can be described as:

$$\mathrm{d}\alpha/\mathrm{d}t = 10^{11.97}(1-\alpha)\mathrm{e}^{-1.90\times10^4/T}.$$

4. Conclusions

Three new neodymium compounds were synthesized and characterized. The crystal structure determinations showed that in **1,** the Nd(III) was coordinated with nine oxygens, forming a distorted tricapped trigonal prism, similar to many nine-coordinate lanthanide compounds; compound **3** is a coordination polymer in which Nd(III), surrounded also by nine oxygens, are bis-bidentately bridged by oxalates in *cis*-configuration to form a 1-D chain structure. The source of oxalate anions in **3** was traced by FT-IR techniques. The thermal stability of **1** from room temperature to 600°C was performed and a decomposition mechanism was put forward. The kinetics of the main decomposition process of **2** showed that the kinetic model function in differential form, apparent activation energy, and pre-exponential constant of this reaction was $1-\alpha$, 157.70 kJ mol^{-1}, and $10^{11.97}$ s^{-1}, respectively.

Supplementary material

CCDC-651744 (**1**) and CCDC-659746 (**3**) contain the supplementary crystallographic data for this article. These data can be obtained free of charge at www.ccdc.cam.ac.uk/conts/retrieving.html or from the Cambridge Crystallographic Data Centre (CCDC), 12 Union Road, Cambridge CB2 1EZ, UK; Fax: +44 1223 336033; Email: deposit@ccdc.cam.ac.uk

Acknowledgment

The authors thank the National Defense Key Laboratory of Propellant and Explosive Combustion of China for the financial support.

References

[1] (a) C.J. Kepert, M.J. Rosseinsky. *Chem. Commun.*, 375 (1999); (b) M. Eddaoudi, D.B. Moler, H. Li, B. Chen, T.M. Reinecke, M. O'Keeffe, O.M. Yaghi. *Acc. Chem. Res.*, **34**, 319 (2001); (c) J. Kido, Y. Okamoto. *Chem. Rev.*, **102**, 2357 (2002).

[2] N. Sakagami, J. Homma, T. Konno, K. Okamoto. *Acta Crystallogr., Sect. C*, **53**, 1376 (1997).

[3] A. Patchornik. *Polym. Adv. Technol.*, **13**, 1078 (2002).

[4] (a) S.M. Kaye. *Encyclopedia of Explosives and Related Items*, Vol. 8, p. 274, U.S. Army ARDEC, Dover, NJ (1978); (b) T.B. Brill, P.J. Brush, K.J. James, J.E. Shepherd, K.J. Pfeiffer. *Appl. Spectrosc.*, **46**, 900 (1991); (c) Z. Meng, R. Hu. *Therm. Anal.*, **45**, 79 (1995); (d) T.B. Brill, T.L. Zhang, B.C. Tappan. *Combust. Flame*, **121**, 662 (2000); (e) Y. Wang, C. Chen, S. Lin. *J. Mol. Struct. Theochem.*, **460**, 79 (1999).

[5] (a) S.S. Yun, J.K. Kim, C.H. Kim. *J. Alloys Compound*, **408–412**, 945 (2006); (b) S.-S. Yun, H.-R. Suh, H.-S. Suh, S.-K. Kang, J.-K. Kim, C.-H. Kim. *J. Alloys Compound*, **408–412**, 1030 (2006); (c) T. Zhang, S. Wang, L. Yang, Y. Sun, J. Zhang, X. Qiao. *Chin. J. Inorg. Chem.*, **22**, 1819 (2006); (d) G. Fang, L. Xu, H. Xiao, X. Ju. *Acta Chim. Sin.*, **63**, 1055 (2005); (e) Y. Yang, T. Zhang, J. Zhang, B. Shao, K. Yu. *Chin. J. Struct. Chem.*, **21**, 321 (2002); (f) J. Song, R. Hu, B. Kang, F. Li. *Thermochim. Acta*, **331**, 49 (1999); (g) J. Song, Z. Chen, H. Xiao, R. Hu, F. Li. *Chin. Sci. Bull.*, **44**, 214 (1999); (h) M.D. Coburn, K.Y. Lee. *J. Heterocycl. Chem.*, **27**, 575 (1990).

[6] (a) F. Zhao, P. Chen, Y. Luo, R. Zhang, S. Li, M. Deng, Y. Zhen. *J. Explos. Propellants*, **26**, 1 (2003); (b) P. Chen, F. Zhao, Y. Luo, R. Hu, Y. Zheng, M. Deng, Y. Gao. *Acta Chim. Sinica*, **62**, 1197 (2004); (c) P. Chen, F. Zhao, Y. Luo, R. Hu, S.G. Gao, Y. Zheng, M. Deng, Y. Gao. *Chin. J. Chem.*, **22**, 1057 (2004).

[7] (a) M. Tanogaki, S. Komura, Japanese Patent no. 06220019 (1994); (b) R. Twieg, A. Azema, K. Jain, Y.Y. Cheng. *Chem. Phys. Lett.*, **92**, 208 (1982); (c) P.R. Driscoll, N.J. Fords. US Patent no. 3495969 (1970).

[8] (a) G. Zhang, J. She, Y. Dou, Q. Zhou, M. Yin. *J. Coord. Chem.*, **61**, 865 (2008); (b) Q. Zhou, G. Zhang, F. Zhao, J. Li, X. Fan. *J. Coord. Chem.*, **61**, 3180 (2008); (c) Q. Zhou, G. Zhang, J. She. *J. Coord. Chem.*, **61**, 2601 (2008). (d) J. She, G. Zhang, F. Zhao, Z. Lei, X. Fan. *Struct. Chem.*, **18**, 373 (2007).

[9] (a) S.W. Czuba. *Zeszyty Nauk. Politech. Wroclaw. Chem.*, **2**, 3 (1955); (b) B. Glowiak. *Zeszyty Nauk. Politech. Wroclaw. Chem.*, **7**, 49 (1961).

[10] (a) G.M. Sheldrick. *SHELXL-97, Program for Crystal Structure Refinement*, University of Göttingen, Göttingen, Germany (1997); (b) SHELXTL-5.03 (PC version), *Program Library for Structure Solution and Molecular Graphics*, Siemens Analytical Instrument Division, Madison, WI (1995).

[11] (a) S. Domínguez, J. Torres, J. González-Platas, M. Hummert, H. Schmann, C. Kremer. *J. Coord. Chem.*, **62**, 108 (2009); (b) H. Chen, J. Li, Z. Sun, Y. Zhu, J. Zhang, Y. Zhao, N. Zhang, X. Lu, L. Liu. *J. Coord. Chem.*, **62**, 294 (2009); (c) Y.-F. Liu, D.-F. Rong, H.-T. Xia, D.-Q. Wang, L. Chen. *J. Coord. Chem.*, **62**, 1835 (2009); (d) W. Chen, Z. Yao, D. Liu, S. Ying, J. Liu. *J. Coord. Chem.*, **62**, 1553 (2009); (e) Q. Gao, C.-Y. Zhang, W.-H. Gao, Y. Wu, Y.-B. Xie, J.-H. Sun. *J. Coord. Chem.*, **62**, 2689 (2009); (f) V. Stilinović, B. Kaitner. *J. Coord. Chem.*, **62**, 2698 (2009).

[12] N. Wang, S.-T. Yue, Y.-L. Liu. *J. Coord. Chem.*, **62**, 1914 (2009).

[13] K.I. Nakamoto. *Infrared and Raman Spectra of Inorganic and Coordination Compounds*, 5th Edn, Wiley, New York (1997).